Heliyon 8 (2022) e10931

Contents lists available at ScienceDirect

Heliyon

journal homepage: www.cell.com/heliyon

Research article

Relationship between M6A methylation regulator and prognosis in patients with hepatocellular carcinoma after transcatheter arterial chemoembolization

Deliang Huang [a], Dejing Huang [b,*]

[a] Department of Interventional Medicine, Yellow River Central Hospital, Zhengzhou, Henan Province, China
[b] Department of Thoracic Surgery, The Second Hospital of Harbin Medical University, Harbin, Heilongjiang Province, China

ARTICLE INFO

Keywords:
TACE
HCC
m6A
ceRNA network

ABSTRACT

Background: Patients with mid-stage HCC (hepatocellular carcinoma) may benefit from transcatheter arterial chemoembolization (TACE). However, patient efficacy varies widely, and the detailed assessment index is unknown. The most general methylation alteration in mRNA (Messenger RNA), N6-methyladenosine (m6A), is controlled by the m6A regulator, which is associated with the emergence of tumors. To include the molecular causes of cancer, competition with ceRNA (endogenous RNA) networks is crucial. However, the exact processes they contribute to TACE HCC remain uncertain. The purpose of this study was tantamount to investigating the possible function of ceRNA networks and m6A regulators in patients with TACE HCC.

Methods: Genes Associated with m6A were discovered using the TACE GEO (Gene Expression Omnibus) dataset. An additional estimate of M6A-associated DEGs (differentially expressed genes) was used to create a predictive response model, which is required. LncRNA-miRNA and miRNA-mRNA interactions were then predicted, the regulatory ceRNA network was set up using Cytoscape software, and target genes were identified using GEPIA online analysis. The connection between immunological checkpoints, immune cell marker genes, and target genes for immune cells was also examined.

Results: The detection of 4 m6A-associated DEGs, the development and evaluation of 2 Machine learning models, and the development of risk models that accurately predicted the response rate of specific patients. Additionally, we obtained two miRNAs (micro RNAs)and six lncRNAs (Long non-coding RNAs), forming an 8-pair ceRNA network, and the target gene LRPPRC deletion of one copy number and gene expression was highly correlated with the amount of Tregs immune cells. LRPPRC was related positively with NRP1, IRF5, and ITGAM and negatively with CCR7 and CD8B among immune cell marker genes. We also discovered that LRPPRC correlates positively with immune checkpoint CD274 cells.

Conclusion: The response of HCC patients to TACE therapy may be predicted using a model based on four gene expression data. We also developed a ceRNA network for TACE HCC related to m6A, which offered suggestions for more research into its molecular processes and possible prognostic indicators.

1. Introduction

In terms of cancer-related mortality worldwide, HCC ranks fourth [1]. About 85–90% of all primary liver cancers are HCC, typically detected at an advanced stage of disease development, and have a low overall survival rate since there are no various therapy options [2]. The BCLC (Barcelona Clinical Liver Cancer) stage system classifies TACE as the first-line therapy for intermediate HCC; response rates at one month following TACE varied amongst trials, varying from 39.6 to 87 percent [3, 4, 5].

N6-methyladenosine (m6A), which predominates in the CDS (coding sequence) and 3′UTR (untranslated region) sections of mRNA, is a methylation alteration that affects mRNA stability, translation efficiency, selective splicing, and localization [6]. M6A has been investigated recently and discovered to take part in the pathophysiology and development of hepatocellular carcinoma [7, 8] It is yet unknown how m6A

* Corresponding author.
E-mail address: hdjdoctor@sina.com (D. Huang).

https://doi.org/10.1016/j.heliyon.2022.e10931
Received 30 May 2022; Received in revised form 2 August 2022; Accepted 29 September 2022

modulators affect HCC patients receiving transarterial chemoembolization treatment.

CeRNAs play a significant role in the initiation and progression of malignancies, and they can be utilized as therapeutic targets or as indicators for diagnosis and prognosis [9]. Recent research has revealed that the ceRNA network has a different function in several cancers, including lung adenocarcinoma, osteosarcoma, laryngeal squamous cell carcinoma, and colon cancer [10, 11, 12, 13]. Previous studies have predicted the relationship between the ceRNA network and HCC immune cell-infiltrating cells [14]. However, the ceRNA network of the m6A-related genes in HCC patients after TACE treatment has not been discovered.

In this study, Data on HCC patients treated with transarterial chemoembolization (TACE) from the GEO database, we systematically analyzed 26 widely reported m6A regulators. The response model of HCC patients treated with TACE was constructed and got four target genes. The ceRNA network further explored the mechanism of target genes.

2. Materials and methods

2.1. Acquisition and pre-processing of gene expression data

The gene expression data of 147 HCC patients treated with TACE were obtained from the GEO(Gene Expression Omnibus) database (https://www.ncbi.nlm.nih.gov/GEO/) (GSE104580, Platform: GPL570). These patients were treated with TACE as the primary treatment, of which 81 were labeled as TACE responders and 66 were labeled as TACE non-responders. RNA was extracted from HCC patients before TACE treatment. Gene ID is converted to Gene Symbol based on the platform annotation file, and multiple Gene Symbols are averaged for gene expression. GEO used principal component analysis (PCA) to observe the consistency of gene expression between groups. In this study, we collected 26 reported m6A methylation regulators. Then, after correcting the data, we extracted the expression levels of these m6A methylation regulators.

TCGA (The Cancer Genome Atlas) database (https://portal.gdc.cancer.gov/) provided data on the miRNA transcriptome of HCC. The UCSC Xena database was used to find clinical information on HCC (https://xenabrowser.net/datapages/?dataset=TCGA-LIHC.survival).

2.2. Differential analyses of m6A-related genes

We used box-line plots to examine the expression levels of m6A methylation regulators in samples from patients with responders and non-responders TACE HCC to investigate better the function of m6A methylation regulators in patients with HCC. Heat and box line plots were created using the R package "limma" to examine the differentially expressed genes in the samples. The cutoff threshold was set to a $P < 0.05$.

2.3. Model selection, construction, and evaluation

2.3.1. Model selection

Based on differential genes, use "caret", "DALEX", "GGploT2", "randomForest", The "KernLab", "pROC" R packages compare linear SVM (support vector machines) and RF (random forest tree models). Method = 'RF' in random forest tree, cross-validation 5 times. Linear support vector machine (SVM) method = "svmRadial", prob. model = TRUE.

2.4. Model construction and evaluation

The RF model was used to screen out the characteristic genes. The non-responders were the train cohort; the responders were the test cohort. The 500 trees were generated by default. After finding out the number of trees corresponding to the point with the littlest error, the disease characteristic gene with an importance score of more than ten was carried out. The model was developed based on the GSE104580 cohort and recorded the import of each gene. We track the genes contained in the model construction and sort the genes according to the importance coefficients returned by the model. The nomogram was built using characteristic genes and 'rms' and 'rmda' R packages to evaluate each patient's response rate. The prediction model calibration curve, decision curve analysis (DCA), and clinical impact curve were used as the leading indicators to evaluate the performance of the model.

2.5. Single genes differential analysis and survival analysis

According to the GEPIA (Gene Expression Profiling Interactive Analysis) database (http://gepia.cancer-pku.cn), differential and survival analysis of m6A-related differential genes were conducted. The threshold was set at $logFC > 0.585$, $P\text{-value} < 0.05$, and normal samples were chosen to Match TCGA normal and GTEx data for the differential analysis. Survival evaluation Axial units were selected as months, and the cutoff-high (percent) and cutoff-low (percent) were both set at 50% for the group cutoff, hazard ratio (HR), and 95 percent confidence interval. The overall survival cutoff value was set to a $P\text{-value} < 0.05$.

2.6. CeRNA network constructions

The starBase online database (http://starbase.sysu.edu.cn) was utilized to calculate the mRNA-miRNA and lncRNA-miRNA interaction pairs. Most mRNA-miRNA pairings predicted by two methods were preserved, and seven bioinformatics algorithms (PITA, RNA22, miRmap, microT, miRanda, Pic Tar, and targescan) were used to predict DEmRNAs targeting DEmiRNAs. We additionally make use of the R language packages "Limma," "reshape2," "ggpubr," and "ggExtra" to further increase the dependability of the interactions. Spearman test was run using the "ggExtra" package to assess the expression correlation within each prediction pair (co-expression analysis), the correlation coefficient was set to $cor < -0.2$, $P\text{-value} < 0.001$ as of the endpoint, and it was decided whether there was a difference in the up-or down-regulation of miRNAs in tumor samples compared to normal samples ($P\text{-value} < 0.001$).

2.7. Relationship between target genes and immune cells

Tumor purity correction was performed using the "scan" and "gene" modules of TIMER2.0 (TIMER2.0, http://timer.cistrome.org/). B cells, CD4+ T cells, CD8+ T cells, neutrophils, macrophages, and dendritic cells are six different kinds of immune cells that are abundantly infiltrated in HCC. Target gene copy quantity and gene expression are related to these immune cell types.

2.8. Correlation of target genes with immune cell marker genes

For spearman correlation analysis, the R packages "limma," "reshape2," "ggpubr," and "ggExtra" was used, and the threshold value was set at $P\text{-value} < 0.05$.

2.9. Correlation of target genes with immune checkpoints

The "gene-corr" module of the TIMER2.0 database (http://timer.cistrome.org) employed Spearman correlation coefficients to assess the association between target genes and immune checkpoint-related genes CTLA4, CD274, and PDCD1.

2.10. Methods

We were using the online bioinformatics tool mentioned above. The majority of the statistical analysis was completed. Correlation analysis was carried out using the spearman correlation coefficient on the remaining data using the R software (Version 4.1.1).

3. Results

3.1. Differential analysis of m6A-related genes

GSE104580 was used to capture the transcription expression profiles of HCC samples treated with TACE (81 responders and 66 non-responders). Ten genes were identified as repetitive when gene expression data and 26 m6A methylation regulators were intersected. These ten gene expression levels were recorded. The responders were in the treatment group, whereas the non-responders were in the control group. These ten genes underwent differential analysis to look for mRNAs that differed significantly between the control and treatment groups. There were a total of four mRNAs that showed differential expression, with the threshold value set at *p-value* < *0.05* (Figure 1). Figure 1A and B's boxplot and heatmap demonstrate that the response group had up-regulated levels of YTHDC2 and IGFBP2, whereas the non-respond group had up-regulated levels of RBM15 and LRPPRC.

3.2. Model constructions

We compared two machine learning models to develop predictive gene models for TACE responses: linear SVM and RF. We use Reverse cumulative distribution of residuals (Figure 2A), Boxplots of residuals (Figure 2B), and the ROC curve (Figure 2C) to assess the reliability of

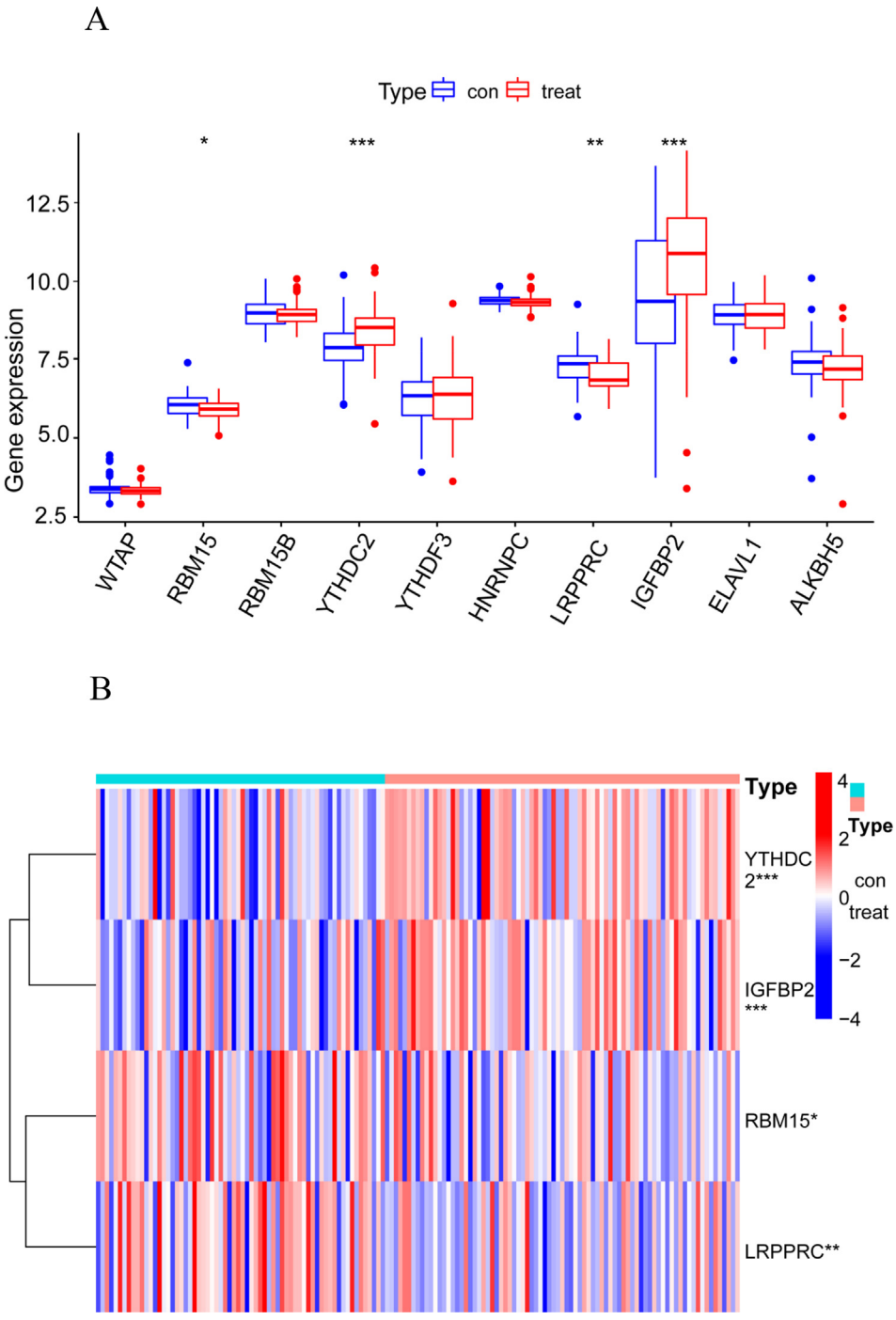

Figure 1. (A). Expression of 10 m6A methylation regulatory factors in RESPONDERS and NO RESPONDERS groups, teat: RESPONDERS, contral: NO RESPONDERS. * *p*-value < 0.05,**p-value < 0.01,***p-value < 0.001.(B). Heatmap of 4 differentially expressed mRNAs. Red indicates high expression, blue indicates low expression.

each model. We found that the RF residue was low, and the AUC of the RF model was 1.000, which was more significant than that of the SVM model (0.856). Finally, RF was a more suitable model for screening disease characteristic genes. The gene expression level of each sample was calculated based on the RF model, and the number of trees corresponding to the point with the minimum error was obtained (Figure 2D). Disease characteristic genes with a critical score more excellent than ten were screened (Figure 2E). The gene expression level of each sample was shown in supplementary document 1.

3.3. Construction and evaluation of individual patient response models

Patient response programs were established based on gene expression levels of YTHDC2, LRPPRC, IGFBP2, and RBM15 in each sample (Figure 3A). The expression levels of different genes in each sample correspond to different points at the top of Figure 3A. Total points were obtained by adding the corresponding points of all genes in each sample. Total points correspond to the corresponding Risk of response to predict the response Risk of a single sample to TACE treatment. The higher the Risk, the higher the response probability and the better the efficacy.

The gap between ideal and bias-corrected lines is exceptionally close, according to calibration curves (Figure 3B). The model's accuracy increases as the distance decreases. Figure 3C's DOC curve demonstrates how distant the m6A genes curve is from the All curve, and the greater the separation between the two lines, the more accurate the model will be. The red curve (Number high risk) in the clinical Impact curve (Figure 3D) indicates the number of individuals identified as positive (high Risk) under the probabilities of each domain. Each domain's number of true positives represents the blue curve (Number high risk with occurrence). Figure 3D's Inclusion of the blue curve in the red curve demonstrates that the sample model we developed can correctly forecast the likelihood that true positives will occur. In conclusion, our model performs well in terms of prediction.

3.4. Single-gene differential analysis and survival analysis

The gene LRPPRC was found to be significantly different between tumor samples and normal samples in the TCGA database, and its expression was up-regulated in the tumor samples. We conducted differential and survival analyses using the GEPIA online database to further validate the model genes' functions (Figure 4A). An examination of survival data revealed that the gene LRPPRC had a significant prognostic risk (*HR= 1.8*) and a bad prognosis (*p-value = 0.00091*) (Figure 4B). To further comprehend its mechanism, we employed the target gene LRPPRC for additional investigation of its ceRNA regulation network.

3.5. LRPPRC (mRNA)-targeted miRNA

In order to further verify the roles of the model genes, we have 64 target miRNAs discovered under the predetermined screening parameters, according to the online starBase database (http://starbase.sysu.edu.cn). Using Cytoscape software, we created an mRNA-miRNA interaction network for enhanced visualization, as seen in Figure 5G. Co-expression study of miRNA and mRNA revealed that two miRNAs (hsa-miR-195-5p and hsa-miR-497-5p) were down-regulated in tumors and adversely correlated with LRPPRC (Figure 5A–D, In respectively).

The samples were split into high and low expression groups for the survival analysis using the best cutoff value, and we found miRNAs (hsa-miR-195-5p and hsa-miR-497-5p) in the low expression group that had worse prognoses (Figure 5E and F).

3.6. lncRNA-targeted miRNAs

Four lncRNAs (HCG18, LINC01703, NutM2A-AS1, and NUTM2A-AS1) were negatively associated with miRNA hsa-miR-195-5p (Figure 6A–D) and were up-regulated in tumor cells (Figure 6E–H) THUMPD3-AS1, according to co-expression analysis and differential analysis of miRNA-lncRNAs. HCG18, NUTM2A-AS1, SNHG16, and

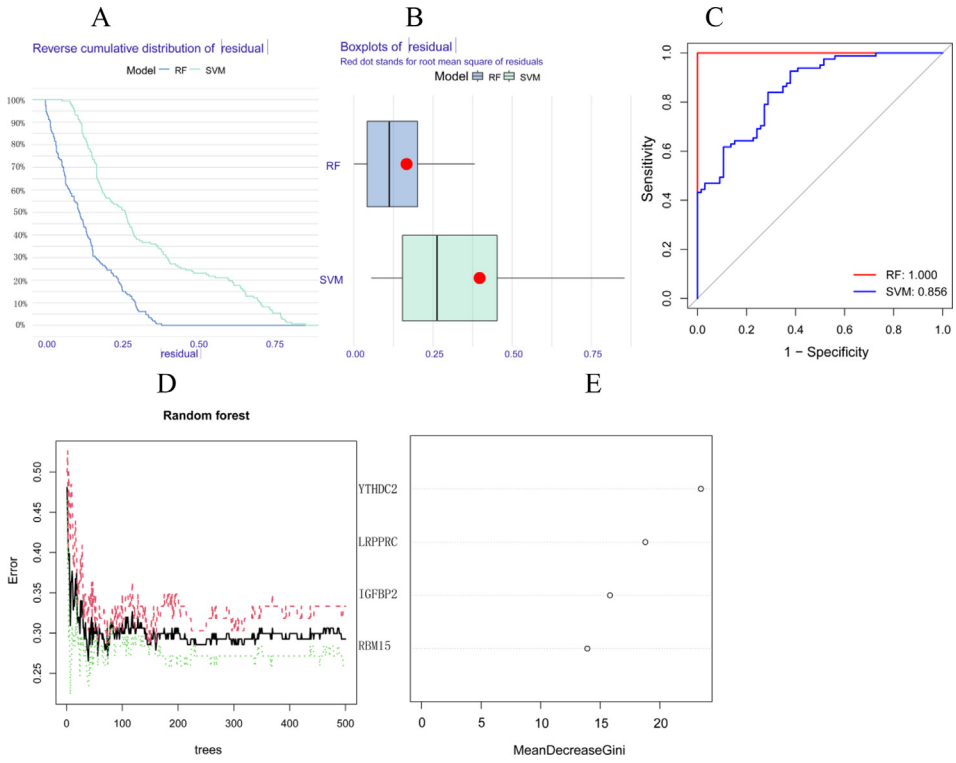

Figure 2. (A, B) Residual. (C) ROC curve. (D) Random Forest. (E) Significance of genes (mRNA) display graph.

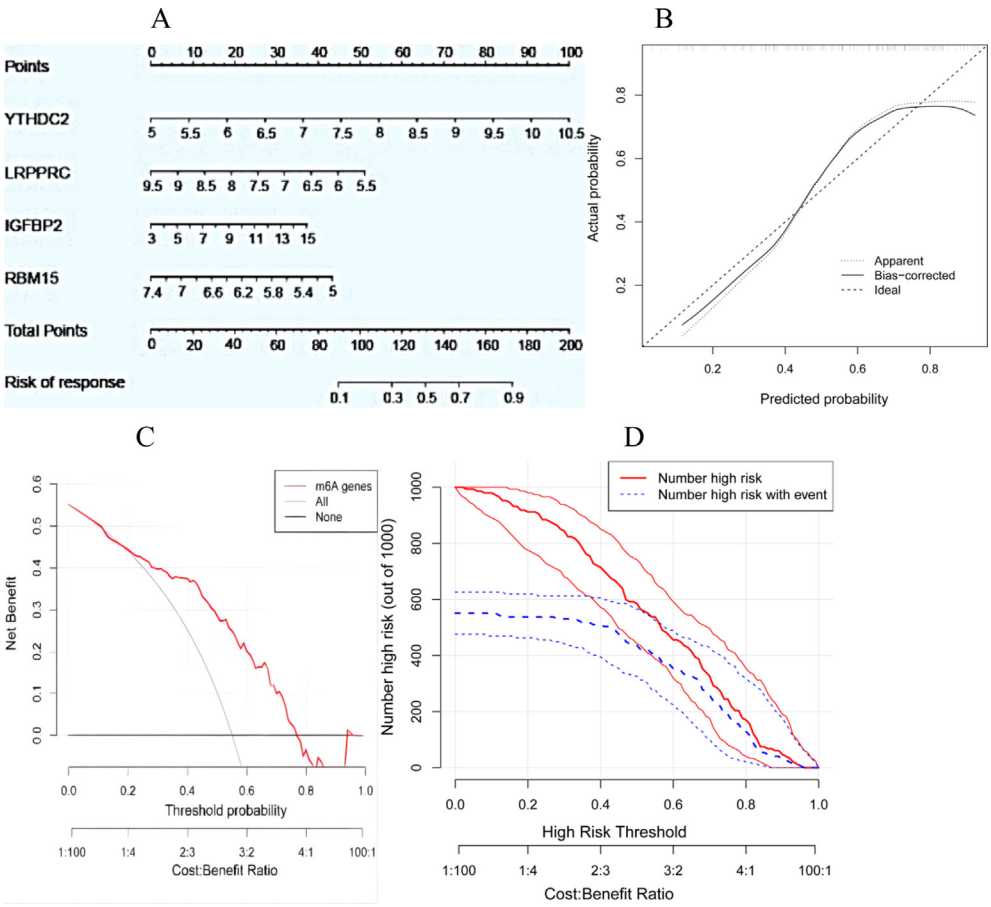

Figure 3. (A) Columnar plot of patient responses. (B) Predictive model calibration curves. (C) DOC curve. (D) Clinical impact curves. The red curve (Number high risk) indicates the number of people classified as positive (high risk) by the model at each domain probability, and the blue curve (Number high risk with event) indicates the number of true positives at each domain probability.

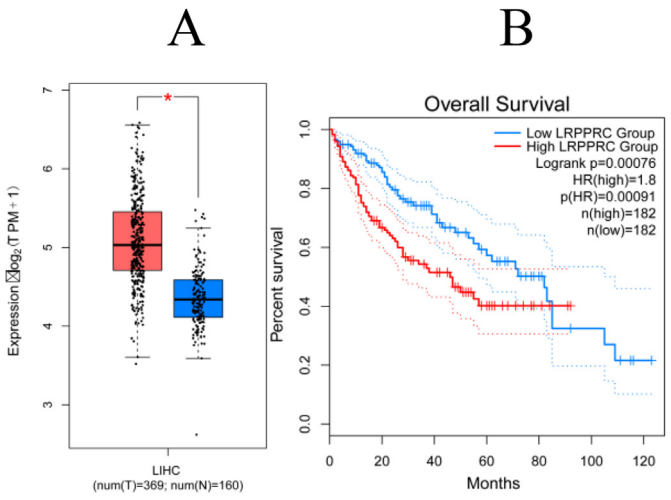

Figure 4. (A) Difference analysis. Normal samples are colored blue and tumor samples are colored red. *p-value < 0.05. (B) Survival analysis: the samples were classified into two groups based on median values. The high expression group is colored in red and the low expression group is colored in blue.

TSPEAR-AS2 were the four lncRNAs negatively correlated with miRNA hsa-miR-497-5p (Figure 6I–L) and up-regulation in tumor cells (Figure 6E, G, M, and N). Lastly, the mRNA LRPPRC and six lncRNAs showed a clear correlation (Figure 6O–T). The samples were sorted into high and low expression groups based on the appropriate cutoff in a survival analysis based on the six lncRNAs. One low expression lncRNA (TSPEARAS2) group and five high expression lncRNA groups (Figure 6U–Y) both showed poor prognoses (Figure 6Z).

3.7. Construction of ceRNA network

Two miRNAs (hsa-miR-195-5p and hsa-miR-497-5p), six lncRNAs (HCG18, LINC01703, NUTM2A-AS1, SNHG16, TSPEAR-AS2, and THUMPD3-AS1) were obtained from the above analysis, constituting eight pairs of ceRNA networks, and the networks were visualized using Cytoscape software (see Figure 7A and B) (see Figure 7A and B). Finally, 8 DEmRNA-DEmiRNA pairs with possible interactions were found.

3.8. Relationship between target genes and immune cells

Online analysis of LRPPRC copy number according to TIMER2.0 was performed with B cells, Tregs, CD4+ T cells, CD8+ T cells, neutrophils, macrophages, dendritic cells (DCs), and follicular helper T cells (Tfh). Compared with the normal copy number, the content of CD8+ T, Tregs, and Tfh in immune cells decreased with one copy number deletion of the LRPPRC gene ($P < 0.05$) (Figure 8A–C); we also evaluated the correlation between LRPPRC gene expression and the eight immune cells, LRPPRC gene expression was correlated with B cells, Tregs, CD4+ T cells, neutrophils, macrophages, and myeloid-derived suppressor cells immune cell content were positively correlated ($Rho > 0, P < 0.05$) (Figure 8D–I).

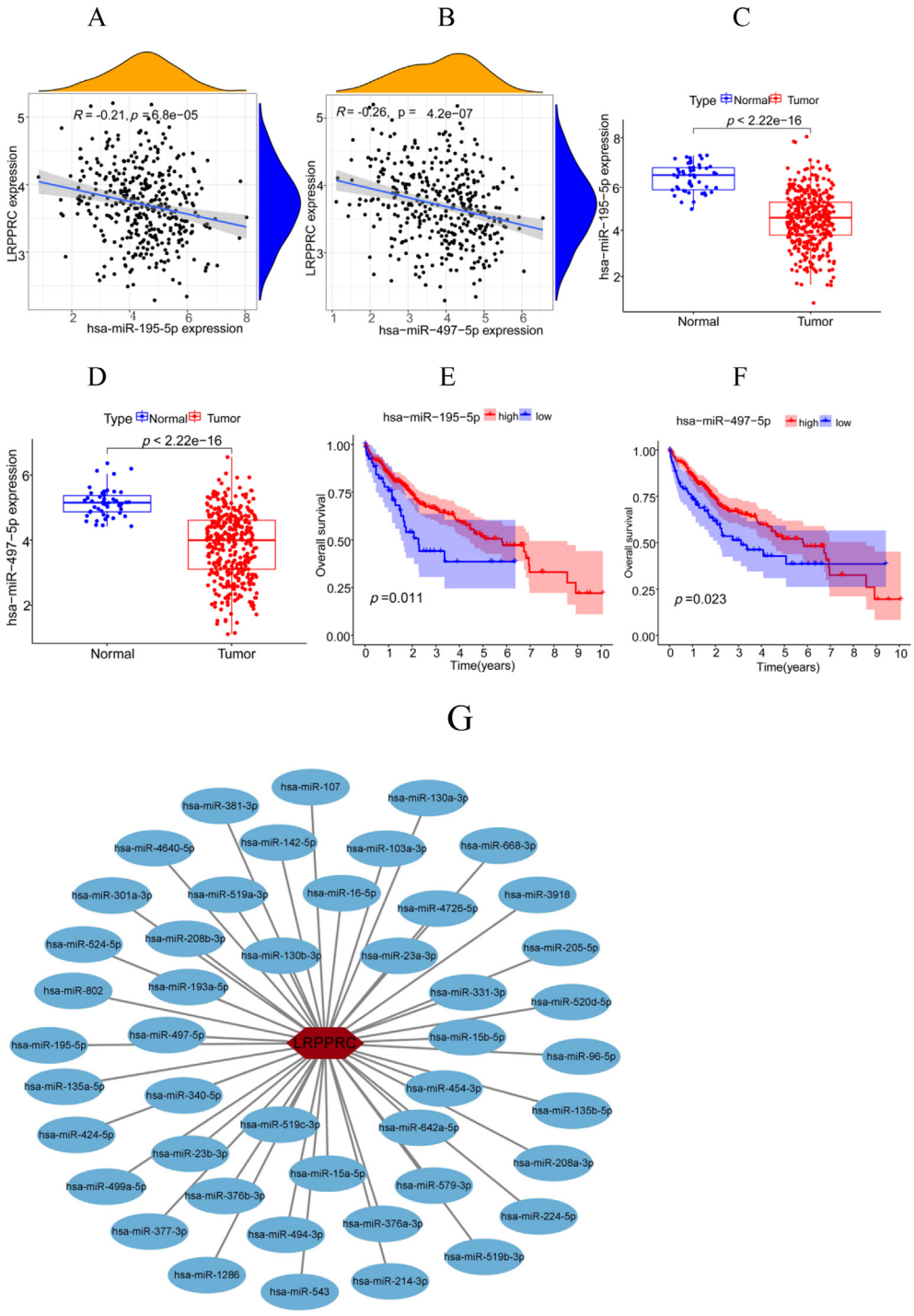

Figure 5. (A) co-expression analysis of hsa-miR-195-5p-LRPPRC. (B) Co-expression analysis of hsa-miR-497-5p-LRPPRC. (C) Differential analysis of hsa-miR-195-5p-LRPPRC. (D) Differential analysis of hsa-miR-497-5p-LRPPRC. (E) Survival analysis of hsa-miR-195-5p. (F) Survival analysis of hsa-miR-497-5p. (G) miRNA-mRNA regulatory network.

3.9. Correlation of target genes with immune cell marker genes

According to the set criteria, we obtained that LRPPRC was positively correlated with NRP1and IRF5 and (*p-value* < *0.05*) (Table 1).

3.10. Target gene and immune checkpoint correlation

Based on the TIMER2.0 database, we obtained that LRPPRC gene expression was positively correlated with CD274 in HCC, and the difference was statistically significant (*rho* > *0, P* < *0.05*) (Figure 9A). LRPPRC gene expression was positively correlated with CTLA4 and PDCD1, but the difference was no statistical significance (Figure 9B and C) (*P* > *0.05*).

4. Discussion

In this study, the subjects were grouped according to responders and non-responders because previous studies showed that the survival rate of responders after TACE was significantly improved (67 months vs. non-responders: 39.5 months, *p* < *0.0001*) [15]. After studying the

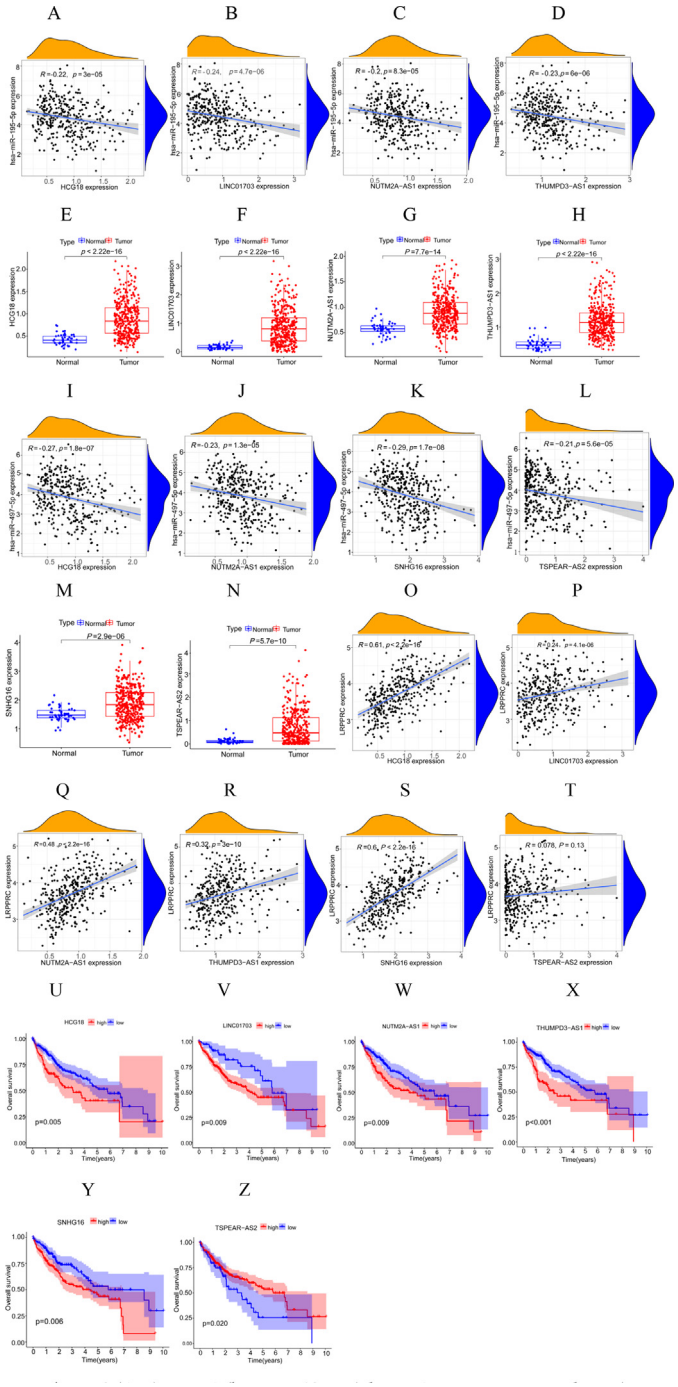

Figure 6. (A–D) miRNA (hsa-miR-195-5p)-lncRNA co-expression analysis. (E–H, M and N) lncRNA expression in tumor samples. Normal samples are indicated in blue and tumor samples are indicated in red. (I–L) miRNA (hsa-miR-497-5p)-lncRNA co-expression analysis. (O–T) LRPPRC-lncRNA co-expression analysis. (U–Z) lncRNA survival analysis. The samples were assigned to two groups based on median values. The high expression group is colored in red and the low expression group is colored in blue.

differences in gene expression between TACE responders and non-responders, we developed a model using four genes (RBM15, LRPPRC, YTHDC2, or IGFBP2) and TACE-specific responses. We can use this model to predict the efficacy of patients after TACE to guide clinical treatment.

In HCC, only a small number of target genes have been studied, most of which are unrelated to TACE. Our study found increased expression of RBM15 and LRPPRC in non-responders. The role of LRPPRC and RBM15 in tumors has been extensively studied. For example, RBM15 was a predictor of OS and DFS in HCC patients and was independently associated with anti-PD-1 immunotherapy response [16]. The prognosis of gastric cancer is significantly affected by the expression of LRPPRC, which is positively correlated with the proliferation of gastric cancer cells [17]. However, the role of LRPPRC in human HCC cells remains unclear. We found that LRPPRC is highly expressed in HCC and has a poor prognosis after TACE treatment. Therefore, this study further explores its mechanism of action.

A family of proteins with PPR patterns that have undergone significant evolutionary conservation includes LRPPRC. PPR proteins cooperate with RNA to mediate translation, splicing, stability, and other RNA-related processes [18, 19].

Treg is naturally present in the immune system, and the activation and proliferation of CD4+ and CD8+ T cells in vitro can be inhibited in various ways in vitro and in vivo [20]. It has been established that the amount of Tregs in the HCC tumor microenvironment is significantly higher than in the normal HCC surrounding tumor tissue and biopsy specimens [21]. We also found a positive correlation with Both copy number deletion and gene expression of LRPPRC correlated with Tregs immune cell content (Figure 8B and E). Combined with previous studies and our studies, we speculated that there was an apparent link between the LRPPRC gene and Tregs and HCC pathogenesis, so we explored the relationship between LRPPRC and immune checkpoint and found that the LRPPRC gene was positively correlated with CD274 in HCC, and the activation of CD274 pathway contributed to tumor immune escape, and blocking this pathway could enhance the endogenous anti-tumor effect of the body. This conclusion again proves the feasibility of immunotherapy. Perhaps this is the future direction of targeted therapy for HCC.

We examined the LRPPRC-associated ceRNA network to investigate the possible mechanisms of LRPPRC in human hepatocellular carcinoma and patients treated with TACE. First, we concluded that LRPPRC expression was elevated in HCC samples and that overexpression suggested a poorer prognosis based on the data in the GEPIA database. We identified two miRNAs linked with prognosis in hepatocellular carcinoma patients, hsa-miR-195-5p and hsa-miR-497-5p, using the starBase online database and miRNA-mRNA co-expression analysis. Gene regulators called microRNAs (miRs) play crucial roles in some carcinogenesis and tumor growth processes. MiR-195-5p expression was downregulated in non-small cell lung and cervical cancer in earlier studies [22, 23] hsa-miR-195-5p was overexpressed in hepatocellular carcinoma cells, and PHF19 expression was reduced, inhibiting cell invasion, migration, and proliferation in vitro [24]. The above findings are in agreement with our study.

After differential analysis and survival analysis of these anticipated lncRNAs, the starBase database predicted lncRNAs binding to hsa-mir-195-5p and hsa-mir-497-5p. Except for TSPEAR-AS2, which was not controlled, we discovered that six lncRNAs (HCG18, LINC01703, NUTM2A-AS1, SNHG16, TSPEAR-AS2, and THUMPD3-AS1) were considerably up-regulated in hepatocellular carcinoma. Other investigations have discovered that HCG18 stimulates hepatocellular carcinoma advancement through the miR-214-3p/CENPM axis and the circulating D1-WNT pathway in head and neck squamous cell carcinoma [25, 26] Similarly, LINC01703 enhances the invasiveness of NSCLC cells by altering Mir-605-3p/MACC1 [27], LncRNA SNHG16 drives the proliferation and invasion of papillary thyroid carcinoma by regulating

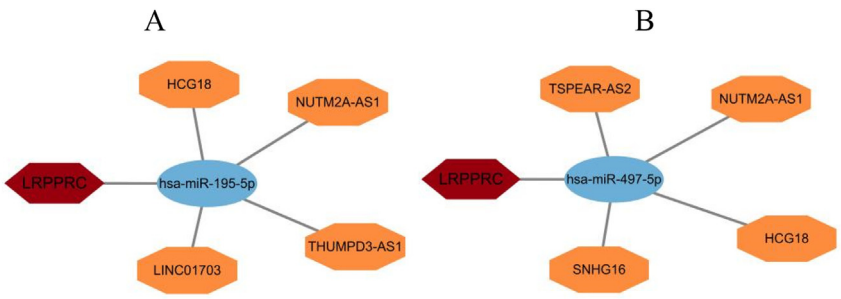

Figure 7. (A, B) mRNA-miRNA-mRNA ceRNA network. Hexagon (red), Ellipse (blue), and Octagon (yellow) represent mRNAs, miRNAs, and lncRNAs, respectively. Gray lines indicate miRNA-mRNA and miRNA-lncRNA interactions.

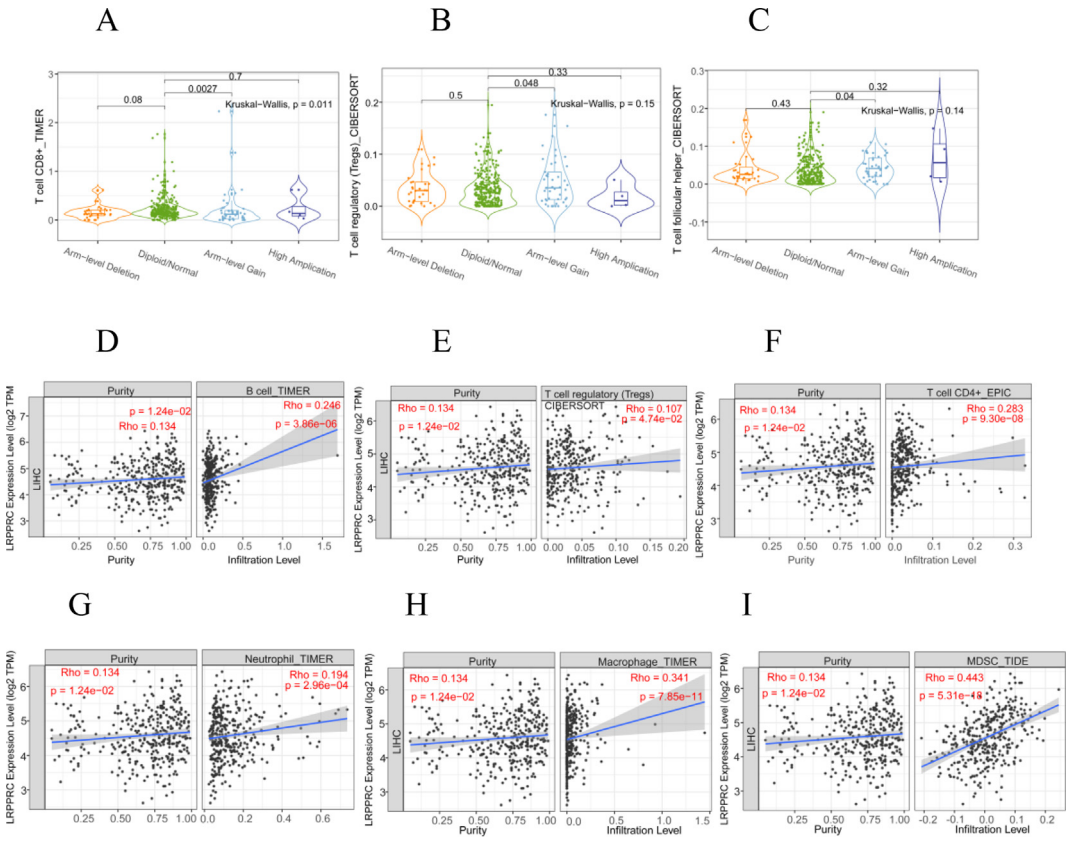

Figure 8. (A–C) Relationship between LRPPRC gene copy number and immune cells. (D–I) Correlation between LRPPRC gene expression and immune cells.

Table 1. Correlation between LRPPRC gene and immune cell marker gene.

immune cells	gene	*cor*	*p-value*
Dendritic cell	NRP1	*0.377478402*	*5.17E-14*
M1 macrophage	IRF5	*0.237282333*	*3.72E-06*

Cor represents the co-expression coefficient, $|cor| > 0.2$, $p < 0.05$ was considered statistically significant.

Mir-497 [28], TSPEAR-AS2, Up-regulation of PPM1A by sponging Mir-487a-3p promotes the progression of oral squamous cell carcinoma [29]. Furthermore, the HSA-Mir-497-5p-NUTM2A-AS1 axis has been verified in recent studies [30]. As a result, it is clear that the mRNAs, miRNAs, and lncRNAs we examined all play a significant part in the cancer stem, and most of these roles have been experimentally verified. Although some of these mRNA-miRNA and miRNA-lncRNA axes have been validated, the ceRNA network made up of mRNA-miRNA-lncRNA has received less research. It is necessary to look at ceRNA networks' intricacy more thoroughly. Therefore, we have every reason to believe that from a clinical and scientific point of view, the eight ceRNAs we have studied are of great significance, not only conducive to the development of new treatment methods, including immunotherapy but also can increase the efficacy of TACE treatment, which is an excellent gospel for patients with HCC.

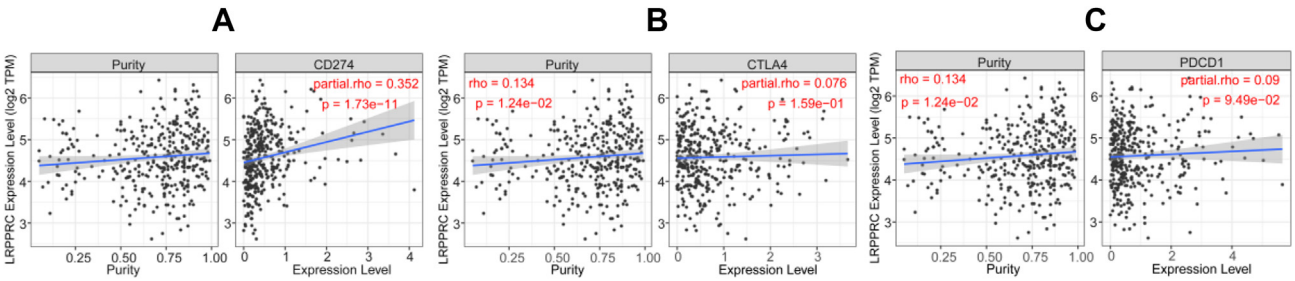

Figure 9. (A–C) Correlation of target genes with immune checkpoints. CD274 (A), CTLA4 (B), PDCD1 (C).

5. Conclusion

In this study, we developed an in-response model for HCC patients receiving TACE and further examined the mechanisms of survival prognosis-related model genes in combination with m6A. This work paves the way for future research on the molecular mechanisms and potential prognostic biomarkers of in-response in patients with hepatocellular carcinoma and HCC receiving TACE. The current study has some drawbacks. In our analysis, a small sample size allowed us to identify just one GEO cohort of HCC patients treated with transarterial chemoembolization (TACE). Furthermore, only the connections between lncRNAs, miRNAs, and genes were examined in this study, and as the regulatory mechanisms of ceRNA networks are pretty complex, additional experimental confirmation is necessary.

Declarations

Author contribution statement

Deliang Huang: Conceived and designed the experiments; Analyzed and interpreted the data; Contributed reagents, materials, analysis tools or data; Wrote the paper.

Dejing Huang: Conceived and designed the experiments; Wrote the paper.

Funding statement

This research did not receive any specific grant from funding agencies in the public, commercial, or not-for-profit sectors.

Data availability statement

All the data were obtained from the public databases.

Declaration of interest's statement

The authors declare no conflict of interest.

Additional information

Supplementary content related to this article has been published online at https://doi.org/10.1016/j.heliyon.2022.e10931.

Acknowledgements

The authors thank the TCGA, UCSC, GEO, Timer2.0, TIDE, StarBase and GEPIA database for allowing them to upload the useful datasets.

References

[1] A. Villanueva, Hepatocellular carcinoma, N. Engl. J. Med. 380 (15) (2019) 1450–1462.
[2] J.D. Yang, L.R. Roberts, Hepatocellular carcinoma: a global view, Nat. Rev. Gastroenterol. Hepatol. 7 (8) (2010) 448–458.
[3] S. Chen, W. Yu, K. Zhang, W. Liu, Comparison of the efficacy and safety of Transarterial chemoembolization with and without Apatinib for the treatment of BCLC stage C hepatocellular carcinoma, BMC Cancer 18 (1) (2018) 1131.
[4] K.C. Albrecht, R. Aschenbach, I. Diamantis, N. Eckardt, U. Teichgraber, Response rate and safety in patients with hepatocellular carcinoma treated with transarterial chemoembolization using 40-microm doxorubicin-eluting microspheres, J. Cancer Res. Clin. Oncol. 147 (1) (2021) 23–32.
[5] K. Bannangkoon, K. Hongsakul, T. Tubtawee, E. McNeil, H. Sriplung, V. Chongsuvivatwong, Rate and predictive factors for sustained complete response after selective transarterial chemoembolization (TACE) in patients with hepatocellular carcinoma, Asian Pac. J. Cancer Prev. APJCP 19 (12) (2018) 3545–3550.
[6] T. Sun, R. Wu, L. Ming, The role of m6A RNA methylation in cancer, Biomed. Pharmacother. 112 (2019), 108613.
[7] Y. Chen, C. Peng, J. Chen, D. Chen, B. Yang, B. He, et al., WTAP facilitates progression of hepatocellular carcinoma via m6A-HuR-dependent epigenetic silencing of ETS1, Mol. Cancer 18 (1) (2019) 127.
[8] L. Zhong, D. Liao, M. Zhang, C. Zeng, X. Li, R. Zhang, et al., YTHDF2 suppresses cell proliferation and growth via destabilizing the EGFR mRNA in hepatocellular carcinoma, Cancer Lett. 442 (2019) 252–261.
[9] X. Qi, D.H. Zhang, N. Wu, J.H. Xiao, X. Wang, W. Ma, ceRNA in cancer: possible functions and clinical implications, J. Med. Genet. 52 (10) (2015) 710–718.
[10] Y. Shi, D. Yang, Y. Qin, Identifying prognostic lncRNAs based on a ceRNA regulatory network in laryngeal squamous cell carcinoma, BMC Cancer 21 (1) (2021) 705.
[11] G. Man, A. Duan, W. Liu, J. Cheng, Y. Liu, J. Song, et al., Circular RNA-related CeRNA network and prognostic signature for patients with osteosarcoma, Cancer Manag. Res. 13 (2021) 7527–7541.
[12] Z. Zhang, W. Qian, S. Wang, D. Ji, Q. Wang, J. Li, et al., Analysis of lncRNA-associated ceRNA network reveals potential lncRNA biomarkers in human colon adenocarcinoma, Cell. Physiol. Biochem. 49 (5) (2018) 1778–1791.
[13] X. Wang, R. Su, Q. Guo, J. Liu, B. Ruan, G. Wang, Competing endogenous RNA (ceRNA) hypothetic model based on comprehensive analysis of long non-coding RNA expression in lung adenocarcinoma, PeerJ 7 (2019), e8024.
[14] J. Zhu, L. Wang, Y. Zhou, J. Hao, S. Wang, L. Liu, et al., Comprehensive analysis of the relationship between competitive endogenous RNA (ceRNA) networks and tumor infiltrating-cells in hepatocellular carcinoma, J. Gastrointest. Oncol. 11 (6) (2020) 1381–1398.
[15] V. Fako, S.P. Martin, Y. Pomyen, et al., Gene signature predictive of hepatocellular carcinoma patient response to transarterial chemoembolization, Int. J. Biol. Sci. 15 (12) (2019) 2654–2663.
[16] H. Jiang, G. Ning, Y. Wang, W. Lv, Identification of an m6A-related signature as biomarker for hepatocellular carcinoma prognosis and correlates with sorafenib and anti-PD-1 immunotherapy treatment response, Dis. Markers 2021 (2021), 5576683.
[17] X. Li, L. Lv, J. Zheng, J. Zhou, B. Liu, H. Chen, et al., The significance of LRPPRC overexpression in gastric cancer, Med. Oncol. 31 (2) (2014) 818.
[18] M.L. Hayes, K. Giang, R.M. Mulligan, Molecular evolution of pentatricopeptide repeat genes reveals truncation in species lacking an editing target and structural domains under distinct selective pressures, BMC Evol. Biol. 12 (2012) 66.
[19] S. Manna, An overview of pentatricopeptide repeat proteins and their applications, Biochimie 113 (2015) 93–99.
[20] S.Z. Josefowicz, L.F. Lu, A.Y. Rudensky, Regulatory T cells: mechanisms of differentiation and function, Annu. Rev. Immunol. 30 (2012) 531–564.
[21] H.Q. Zhao, W.M. Li, Z.Q. Lu, et al., Roles of Tregs in development of hepatocellular carcinoma: a meta-analysis, World J. Gastroenterol. 20 (24) (2014) 7971–7978.
[22] S.Z. Josefowicz, L.F. Lu, A.Y. Rudensky, Regulatory T cells: mechanisms of differentiation and function, Annu. Rev. Immunol. 30 (2012) 531–564.
[23] S.S. Pan, H.E. Zhou, H.Y. Yu, L.H. Xu, MiR-195-5p inhibits the cell migration and invasion of cervical carcinoma through suppressing ARL2, Eur. Rev. Med. Pharmacol. Sci. 23 (24) (2019) 10664–10671.
[24] H. Xu, Y.W. Hu, J.Y. Zhao, X.M. Hu, S.F. Li, Y.C. Wang, et al., MicroRNA-195-5p acts as an anti-oncogene by targeting PHF19 in hepatocellular carcinoma, Oncol. Rep. 34 (1) (2015) 175–182.
[25] B. Mao, F. Wang, J. Zhang, Q. Li, K. Ying, Long non-coding RNA human leucocyte antigen complex group-18 HCG18 (HCG18) promoted cell proliferation and migration in head and neck squamous cell carcinoma through cyclin D1-WNT pathway, Bioengineered 13 (4) (2022) 9425–9434.
[26] Y. Zou, Z. Sun, S. Sun, LncRNA HCG18 contributes to the progression of hepatocellular carcinoma via miR-214-3p/CENPM axis, J. Biochem. 168 (5) (2020) 535–546.

[27] Y. Wang, J. Fu, Z. Wang, Z. Lv, Z. Fan, T. Lei, Screening key lncRNAs for human lung adenocarcinoma based on machine learning and weighted gene co-expression network analysis, Cancer Biomarkers 25 (4) (2019) 313–324.
[28] Q. Wen, L. Zhao, T. Wang, N. Lv, X. Cheng, G. Zhang, et al., LncRNA SNHG16 drives proliferation and invasion of papillary thyroid cancer through modulation of miR-497, OncoTargets Ther. 12 (2019) 699–708.
[29] Y.C. Xia, J. Cao, J. Yang, Y. Zhang, Y.S. Li, lncRNA TSPEAR-AS2, a novel prognostic biomarker, promotes oral squamous cell carcinoma progression by upregulating PPM1A via sponging miR-487a-3p, Dis. Markers 2021 (2021), 2217663.
[30] J. Zhang, W. Lou, A key mRNA-miRNA-lncRNA competing endogenous RNA triple sub-network linked to diagnosis and prognosis of hepatocellular carcinoma, Front. Oncol. 10 (2020) 340.